Journal of Catalysis 266 (2009) 120–128

Contents lists available at ScienceDirect

Journal of Catalysis

journal homepage: www.elsevier.com/locate/jcat

The role of different Ni sites in supported nickel catalysts for butene dimerization under industry-like conditions

A. Brückner [a,*], U. Bentrup [a], H. Zanthoff [b], D. Maschmeyer [c]

[a] Leibniz-Institut für Katalyse an der Universität Rostock e. V., Albert-Einstein-Str. 29a, D-18059 Rostock, Germany
[b] Evonik Degussa GmbH, Paul-Baumann-Str. 1, D-45772 Marl, Germany
[c] Evonik Oxeno GmbH, Paul-Baumann-Str. 1, D-45772 Marl, Germany

ARTICLE INFO

Article history:
Received 24 February 2009
Revised 13 May 2009
Accepted 31 May 2009
Available online 23 June 2009

Keywords:
Supported Ni catalysts
Butene oligomerization
Operando EPR
In situ FTIR
CSTR tests

ABSTRACT

An industrial 20% NiO/SiO_2–Al_2O_3 catalyst and model systems prepared by impregnation of two differently acidic SiO_2–Al_2O_3 supports with $Ni(Cp)_2$ or $Ni(COD)_2$ have been analyzed by spectroscopic in situ studies and catalytic CSTR tests during butene oligomerization under industrially relevant conditions. Active and selective sites for linear C_8 target olefins are single Ni^{n+} species ($n = 1$ and/or 2) which form during conditioning by oxidative addition of Brønsted sites to Ni^0 precursor species. This is connected with a switch from an acid-catalyzed ionic mechanism to a metal-catalyzed coordinative mechanism, which shifts the product composition from strongly branched olefins to more linear olefins. Deactivation at extended times on stream is due to reaggregation of the active Ni single sites to Ni^0 clusters. Operando EPR performed for the first time in flowing butenes at 20 bar clearly shows that such clusters are not active. Brønsted sites play a crucial role in stabilizing the Ni single sites.

1. Introduction and objective

Since about 60 years [1], even more than a decade before the detection of the so-called "nickel effect" by Ziegler, nickel-containing catalysts are being used for the oligomerization of n-butenes in both homogeneous and heterogeneous catalytic processes. While the homogenous DIMERSOL™ process is performed over nickel complexes in the presence of organo-aluminium activators as catalysts, the heterogeneous OCTOL™ process is performed over supported NiO/Al_2O_3–SiO_2 catalysts at reaction temperatures of 343 to 393 K in the liquid phase using the C_4 fraction from the steam cracker (raffinate III) as feedstock [2]. The product composition strongly depends on the surface acidity of the catalysts. Highly acidic catalysts with a low Ni/Al ratio preferentially produce undesired strongly branched products such as dimethylhexenes and higher oligomers via a carbenium ion mechanism, while materials with a lower acidity (higher Ni/Al ratio) show a high selectivity to the target products n-octenes and methylheptenes [3].

Over optimized catalysts, on which a Ni-catalyzed coordinative mechanism is predominant, typical C_8 selectivities of ≈80% are obtained at a conversion of ≈45% to 47%, and the C_8 fraction consists typically of 13% n-octenes, 62% methylheptenes and 25% dimethylhexenes [2]. However, it has also been shown that the behaviour of the supported NiO/Al_2O_3–SiO_2 catalysts is strongly dynamic, especially within the first several hours on stream. The product composition in the initial reaction period reflects a predominating carbenium ion mechanism with a high dimethylhexene selectivity which is gradually replaced by a metal-catalyzed mechanism leading to far more linear products in due course [4]. This suggests that during the conditioning period the nature of the active sites may change too, yet little is known about this change.

The product composition over optimized supported NiO/Al_2O_3–SiO_2 catalysts is very similar to that obtained in the homogeneous butene dimerization process [4]. This suggests that the reaction mechanism and the properties of active Ni sites might also be similar in both cases. In general, a Ni^+–H species is considered to be the active site in the homogeneous olefin oligomerization process in which two butene molecules are inserted subsequently and the final olefin product is eliminated by β-H elimination which is assumed to restore the active Ni^+–H species [5–8].

For heterogeneous catalysts, the structure and valence state of the active nickel sites as well as the mechanism of their formation from precursor species are still not well understood. In early studies of supported NiO/Al_2O_3–SiO_2 catalysts, a layered nickel aluminosilicate was suggested as the active phase with coordinatively unsaturated Ni^{2+} as the active sites [9]. In Ni-exchanged Y zeolites, Ni^+ and superparamagnetic Ni^0 species were detected by EPR spectroscopy after interaction of the zeolite with 1-butene [10], from which it was concluded that either Ni^+ or both these species could be the active sites in olefin oligomerization. EPR-active Ni^+ sites were also detected in prereduced NiCaY zeolites, and a linear relation was

* Corresponding author. Fax: +49 381 1281 51244.
E-mail address: angelika.brueckner@catalysis.de (A. Brückner).

0021-9517/$ - see front matter © 2009 Elsevier Inc. All rights reserved.
doi:10.1016/j.jcat.2009.05.021

found between their concentration and the conversion in ethylene oligomerization [11]. In situ EPR studies of NiCaX and Ni/SiO_2 catalysts in the presence of C_2–C_6 linear olefins have shown that the latter adsorb on Ni^+, shifting the parallel component of the g tensor to values below 2.0 [12]. This was also found for a supported 10 mol% NiO/Al_2O_3–SiO_2 catalyst after pretreatment in vacuum and adsorption of up to 80 kPa of different butenes at 470 K. The resulting EPR signals were assigned to Ni^+–butene complexes. Based on these results, Ni^+ was claimed to be the active site in butene oligomerization [13]. Reduction to Ni^+ was also detected in supported $NiSO_4/\gamma$-Al_2O_3 both after evacuation at 873 K and after interaction of the prereduced catalysts with ethylene or propylene at room temperature. Interestingly, no Ni^+ was detected upon interaction with 1-butene, therefore Ni^+ was excluded as the active site for butene oligomerization [14]. Finally, it should be mentioned that highly dispersed Ni^0 was also suggested as the active site in oligomerization of ethylene over NiY catalysts [15].

It is the aim of this work to shine light upon the way of the formation of Ni^+ and Ni^0 sites in supported nickel catalysts and their role in the heterogeneous n-butene oligomerization process. Therefore, the catalytic reaction has been studied in a continuous stirred tank reactor (CSTR) containing the bare support, while the active catalyst was created in situ by stepwise dosage of the Ni component. For the first time, operando high-pressure EPR measurements of working catalysts have been performed under reaction conditions as close as possible to those of the industrial process to monitor the behaviour of Ni^0 clusters, while Ni^+ was analyzed in catalysts quenched after different times on stream at 77 K. Moreover, the influence of acidic sites on the structure of Ni species was analyzed by in situ FTIR spectroscopy. By integrated evaluation of catalytic and spectroscopic results, detailed knowledge on the desired and detrimental properties of these catalysts should be obtained, which can help to improve their catalytic performance, in particular, the selectivity to linear C_8 products.

2. Experimental

2.1. Catalysts

An industrial NiO/SiO_2–Al_2O_3 catalyst with 20 wt.% NiO (NiO/SiAl-1) prepared by the precipitation of nickel carbonate on an acidic silica-alumina support (SiAl-1, Si:Al ~ 6) followed by subsequent calcination in a N_2 flow at 873 K was obtained from Oxeno. The same SiAl-1 support as well as a silica–alumina support with a lower acidity (SiAl-2, Si:Al ~ 20) was used for the in situ formation of the active catalyst during the CSTR tests by stepwise dosage of solutions of bis-cyclopentadienyl nickel, $Ni(Cp)_2$, or bis-cyclooctadienyl nickel, $Ni(COD)_2$, as well as for the preparation of catalysts for spectroscopic studies. For in situ EPR studies, the support materials were pressed into tablets, crushed, and sieved to obtain particle fractions of 0.3 to 0.8 mm diameter, which were heated for 2 h in dry H_2 and for further 3 h in dry air flow at 873 K to remove impurities. The thus-pretreated supports were transferred into a glove box, impregnated with solutions of $Ni(Cp)_2$ or $Ni(COD)_2$ in dry heptane to achieve Ni loadings of 0.05 to 6.0 wt.% and dried by volatilization of the solvent overnight at room temperature. The thus-prepared catalysts are labelled in due course as *x*Ni/SiAl–*y*(C), where *x* denotes the Ni loading in wt.%, *y* = 1 or 2 refers to the kind of the support and C=Cp or COD indicates the nickel source. For in situ FTIR studies, self-supporting wafers of the supports pretreated at 873 K in H_2 and air flow were heated again for 10 min in vacuum at 673 K within the FTIR cell. The cell was then transferred to the glove box, and the wafers were removed and impregnated with the Ni complex solution. After drying in the glove box at room temperature for a short period , the wafers were remounted into the FTIR cell. Prior to the respective experiments, the residual heptane was removed by evacuation of the FTIR cell at room temperature.

2.2. CSTR experiments

Twenty-five grams of the powdered Ni-free support were dispersed in about 200 ml of butane in a completely flooded CSTR. The catalyst was retained by a fine filter membrane installed so close to the stirrer blades that the formation of a filter cake was prevented by the high shear. The liquid phase was exchanged at a rate of 5 ml/min resulting in a residence time of about 40 min. Ideal CSTR behaviour of the equipment had been verified previously by monitoring with alkane exchange. As feedstock dry raffinate III was used (typical composition: 0.1% isobutene, 19.6% n-butane, 30.5% trans-butene, 14.2% cis-butene, 35.2% 1-butene and 0.19% isobutene). $Ni(Cp)_2$ or $Ni(COD)_2$solutions (1% in heptane) were dosed into the feed stream in 8 ml portions every 10 min via a dosage slope. The composition of the effluent was analyzed every 30 or 60 min for oligomerisates by liquid dosage to a hydrogenating GC equipped with a DB-1 capillary column (Agilent Nr. 127-1013-E, 10 m × 0.1 mm) and a Pt catalyst in the injector section. For C4 analysis, the stream was evaporated and injected into a 30 m × 0.25 mm HP-Al/S capillary column as a gas to prevent column plugging by highly boiling components.

2.3. EPR measurements

Operando EPR measurements were performed using ca. 100 mg of catalyst particles placed in a tubular quartz plug-flow reactor having a 2.5-mm inner diameter and 1.5-mm wall thickness which was directly implemented in the cavity of a Bruker ELEXSYS 500-10/12 cw-EPR spectrometer and connected by Swagelok fittings to a liquiflow meter at the inlet and a pressure controller at the outlet for maintaining a pressure of 20 bar inside the reactor. Heat was transferred to the reactor by a preheated stream of nitrogen [16]. The catalyst was heated in a dry N_2 flow for 10 min at 353 K before pressurizing at this temperature with 20 bars of the reactant mixture.

The same raffinate III mixture as in the CSTR tests was also used as the reactant feed in the operando EPR experiments. This mixture was passed over molecular sieve 5 A to remove traces of moisture before allowing it to enter into the reactor. In a typical run, 1.9 to 2.0 g/h of raffinate III was passed over 80 to 100-mg catalyst particles at 353 K for several hours, and spectra were recorded at this temperature after different time intervals. The product mixture leaving the reactor was expanded to normal pressure and passed through a cold trap at 273 K. The C_4 hydrocarbons not condensed in the cold trap were analyzed by on-line GC. The C_8 olefins were collected in the cold trap for distinct periods of time and analyzed off-line. The same conditions as for the analysis of the CSTR products have been used.

For detecting Ni^+ species, the reaction was stopped after different periods of time by cooling to room temperature and expanding to normal pressure. The reactor was transferred to the glove box, and the catalysts were filled into normal EPR tubes, sealed and measured at 77 K using a finger dewar filled with liquid nitrogen.

Computer simulation of EPR spectra was performed with the program SIM14S of Lozos et al. [17] using the spin Hamiltonian

$$H = \mu_B \cdot S \cdot g \cdot B_0 \quad (1)$$

where μ_B is the Bohr magneton, S is the electron spin operator, g is the g tensor and B_0 is the magnetic field vector.

2.4. FTIR measurements

The surface acidity of the catalysts was studied by FTIR spectroscopy of adsorbed pyridine. Spectra of the self-supporting wafers impregnated with the Ni complex in the glove box were recorded using a Bruker IFS 66 spectrometer equipped with a heatable and evacuable reaction cell with CaF_2 windows, which is connected to gas-dosing and evacuation systems. Prior to pyridine adsorption, the samples were evacuated at room temperature. Pyridine was adsorbed at room temperature, followed by evacuation and heating to 373 K to remove physisorbed pyridine. Spectra were recorded at different temperatures in the range of 373 to 673 K with 2 cm^{-1} resolution and 100 scans.

3. Results

3.1. EPR studies of catalysts with high Ni content

The EPR spectrum of the industrial NiO/SiAl-1 catalysts in N_2 flow at 353 K showed a signal at an effective *g*-value of 2.3, being characteristic of ferromagnetic Ni^0 particles [18], which might have been formed during calcination in N_2 flow upon partial reduction of NiO (Fig. 1A). When pressurizing the catalyst with 20 bar flowing raffinate III, this signal virtually did not change during the first 4.5 h on stream. During this time the catalyst did not show any activity (Fig. 1B). Induction periods of several hours were observed for all the catalysts studied. Since the system was extremely sensitive to water, an induction period was obviously needed to remove traces of adsorbed water and/or other impurities from the catalyst surface which were not completely removed by the pretreatment. After 4.5 h, the onset of activity was evident from the growing relative area of the 2-butene peaks at the expense of 1-butene indicating isomerization. Since n-butane does not react under these conditions, it was used as an internal standard, and the peak areas were normalized on that of n-butane. Along with the onset of activity, the Ni^0 EPR signal decreased (Fig. 1A).

In contrast to NiO/SiAl-1, the EPR signal of ferromagnetic Ni^0 clusters was not yet present in the fresh 6.0Ni/SiAl-1(Cp) catalyst, but it raised quickly upon exposure to raffinate III at 20 bar (Fig. 2A). It reached its maximum intensity after about 90 min and remained constant in due course. However, the catalyst became active only after 300 min as evident from the changing C_4 product composition (Fig. 2B). This clearly shows that ferromagnetic Ni^0 clusters were not responsible for the catalytic activity.

3.2. CSTR experiments

To study the influence of nickel on the catalytic performance in more detail, CSTR tests were performed, in which the active catalyst was formed in situ by stepwise dosage of very low amounts of Ni. CSTR results obtained at a reaction temperature of 353 K using the highly acidic support SiAl-1 are shown in Fig. 3. During the first 120 h, the bare SiAl-1 support was stirred at constant conditions until conversion and selectivity were stationary for a long period. In this initial period, in which no Ni was present, almost exclusively dimethylhexenes (detected by GC as hydrogenated product dimethylhexane) were produced. This agrees with a carbenium ion mechanism proposed for strongly acidic catalysts. After 120 h, the first dosage series was started with 8-ml portions of a 1% $Ni(COD)_2$/heptane solution, resulting in a final Ni content of about 3000 ppm. Right after the start of the first dosage, the product composition analyzed by GC after hydrogenation changed drastically. Now, 3-methylheptane was the major product and n-octane, which was negligible before adding Ni, was observed in a reasonable concentration. After 140 h, the second Ni dosing series was started up to a final Ni content of about 8000 ppm. A sudden

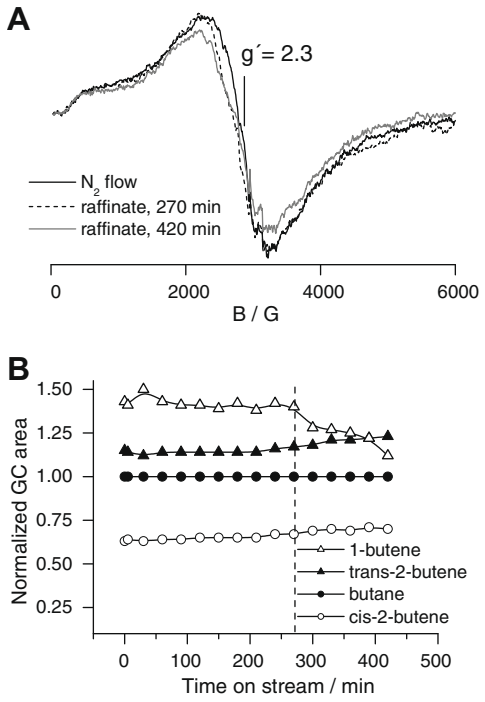

Fig. 1. (A) Operando EPR spectra of NiO/SiAl-1 measured at 353 K in N_2 flow and under 20 bar raffinate III and (B) on-line GC analysis of the C_4 fraction plotted as relative peak areas $A/A_{n\text{-butane}}$.

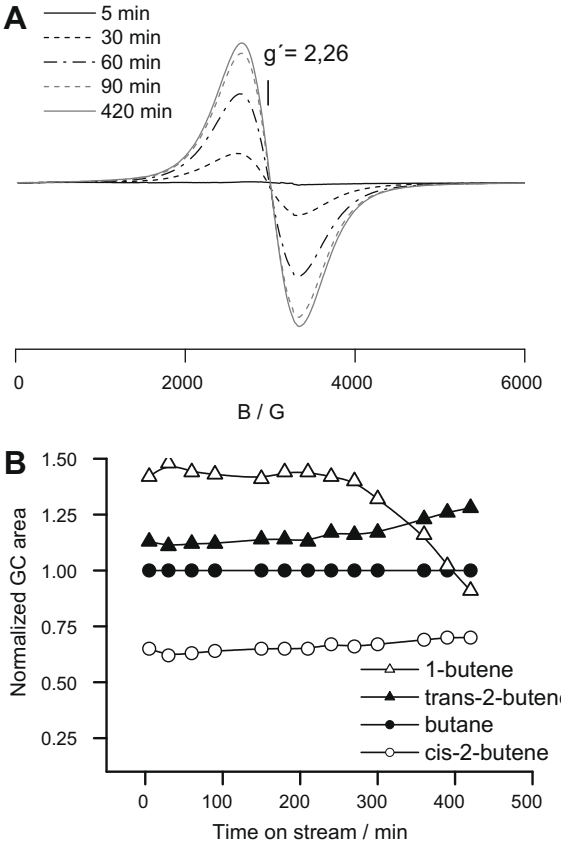

Fig. 2. (A) Operando EPR spectra of 6.0Ni/SiAl-1(Cp) at 353 K under 20 bar raffinate III after different times on stream and (B) on-line GC analysis of the C_4 fraction plotted as relative peak areas $A/A_{n\text{-butane}}$.

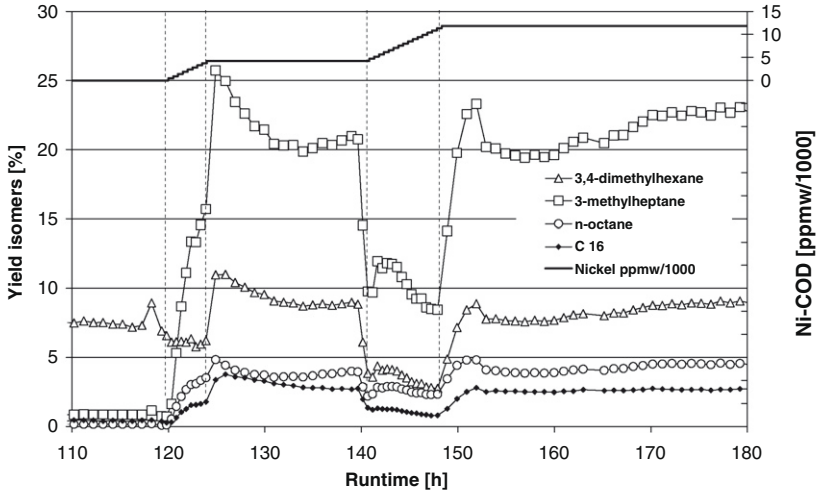

Fig. 3. Activation study of the support SiAl-1 in CSTR at 353 K with stepwise dosage of 1% $Ni(COD)_2$/heptane. The nickel content refers to the mass of silica–alumina. The first dosage series starts at 120 h, and the second at 141 h.

activity loss was observed right after dosing the first portion of the $Ni(COD)_2$ solution. This may be due to the blocking of active sites by COD which was being removed quickly from the CSTR after the dosage was stopped. Then the performance of the catalyst returned to the same level established before starting the second dosing series, indicating that the additional nickel supplied during the second dosage series had no additional effect on the catalyst activity.

In a second experiment, the weakly acidic SiAl-2 carrier was treated with a 1% $Ni(Cp)_2$/heptane solution in the same manner (Supplementary material, Fig. S1). The activation by the Ni dosage was similarly evident as for $Ni(COD)_2$. However, the system did not respond immediately to the addition of nickelocene, but it responded with a marked time delay of nearly 9 h. This may be due to the fact that $Ni(Cp)_2$ is more stable than $Ni(COD)_2$ and needs time to get rid of the Cp ligands. In contrast to the highly acidic SiAl-1 support, the overall activity of the catalyst based on the weakly acidic SiAl-2 support was markedly lower. Moreover, fast deactivation was observed, which was only partially and temporarily compensated by rising the reaction temperature to 373 K.

3.3. EPR studies of catalysts with a low Ni content

For a more detailed analysis of the effect of small Ni loadings observed in the CSTR experiments, in situ EPR experiments were performed using a series of catalysts with a much smaller Ni loading, which were prepared by impregnating the SiAl-1 support with heptane solutions of either $Ni(Cp)_2$ or $Ni(COD)_2$ in which nickel takes the formal valence state of +2 or 0, respectively.

The EPR spectra of the 0.3Ni/SiAl-1(Cp) and 0.3Ni/SiAl-1(COD) catalysts were very different. Even at this low Ni loading, a strong signal of ferromagnetic Ni^0 clusters was observed for the latter sample, while this was not the case for 0.3Ni/SiAl-1(Cp) (Fig. 4A). The small signal around 1500 G ($g \approx 4.3$) was due to a Fe^{3+} impurity in the support. In the middle field range, additional signals appeared which can be assigned to Ni^+ single sites [10–14,19] (Fig. 4B). For 0.3Ni/SiAl-1(Cp), the experimental spectrum can be simulated by superimposing two signals with different g tensor components: (1) $g_1 = 2.081$, $g_2 = 2.025$, $g_3 = 1.911$ and (2) $g_\perp = 2.009$, $g_\parallel = 2.077$. The g tensor values of Signal 1 are very similar to those observed for Ni^+ sites in different supported Ni catalysts such as NiCaX, Ni/SiO_2 and $NiSO_4/\gamma\text{-}Al_2O_3$ after adsorption of different olefins such as ethylene, propylene and different butenes [10–14]. It is also comparable to the signal of the complex

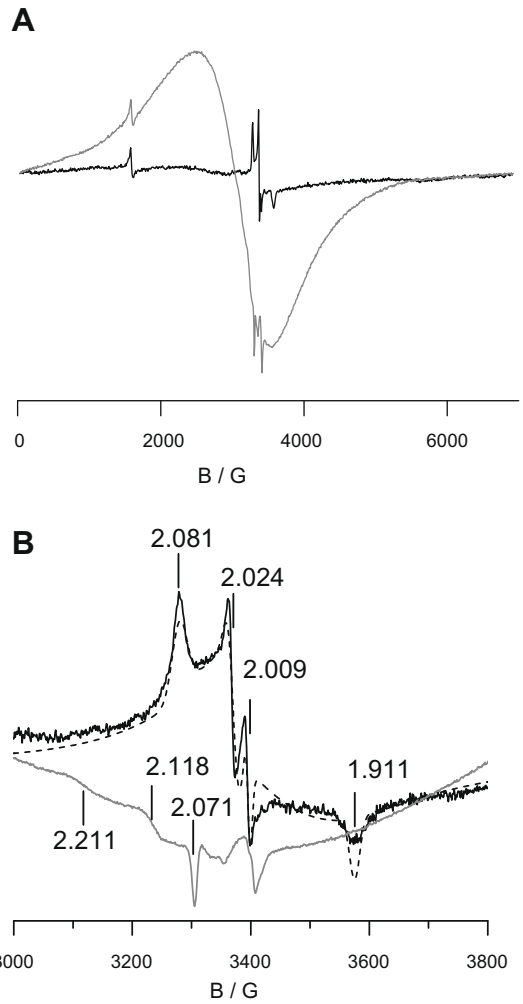

Fig. 4. EPR spectra of fresh 0.3Ni/SiAl-1(Cp) (black) and 0.3Ni/SiAl-1(COD) (gray). Plot B shows the enlarged middle field range of plot A. The dashed line represents the calculated spectrum.

$[(PPh_3)Ni(\eta^2\text{-}C_2H_4)_2]BF_4$ in frozen toluene solution [20]. The common peculiarity of all these spectra is the unusually low g_3 value. According to theory, all g tensor components of Ni^+ (d^9) should

be larger than 2.0023, the g-value for the free electron [19]. The low field shift of g_3 was speculated by some authors to result from the interaction of the Ni d-electrons with the π-electrons of the olefin ligands [11]. For a $[(bpy)Ni(mesityl)_2]^-$ complex showing a similar signal in frozen solution, it was concluded that the electron density is partially shifted from Ni into the π^* orbitals of the ligands [21].

Considering these results, it is not unlikely that the shift of g_3 to 1.911 in the spectrum of 0.3Ni/SiAl-1(Cp) in the absence of raffinate III (Fig. 4B) may arise from the interaction of the Ni d-electrons with the π orbitals of the Cp ligands, suggesting that Cp is still bound to Ni after impregnation. Signal 2 with $g_\perp = 2.009$ and $g_\parallel = 2.077$ in the spectrum of 0.3Ni/SiAl-1(Cp) in Fig. 4B could arise from O_2^- species formed from traces of O_2 being present in the system. When the as-prepared catalyst was exposed to air, this signal was stable while the Ni^+ signal disappeared immediately due to oxidation to Ni^{2+}.

A signal of Ni^+ was also observed for 0.3Ni/SiAl-1(COD). However, in this case, all g tensor components were larger than $g_e = 2.0023$, as expected for Ni^+ (Fig. 4B). Obviously, $Ni(COD)_2$ as a Ni^0 compound is less stable than $Ni(Cp)_2$ when it is adsorbed on the acidic SiAl-1 support and decomposes readily by release of both COD ligands.

To elucidate relations between the nature of Ni sites and the catalytic behaviour, a series of experiments at 353 K under 20 bar of flowing raffinate III were performed with catalysts containing 0.2 to 0.3 wt.% of Ni on the SiAl-1 support. The catalysts were quenched after different times on stream for analyzing the state of Ni by EPR at 77 K. These spectra together with the composition of the C_8 product fraction are displayed in Figs. 5 and 6.

The spectrum of the fresh 0.3Ni/SiAl-1(COD) catalyst in Fig. 5 shows a signal of single Ni^+ sites similar to that in Fig. 4. This line was not observed anymore after Experiments 2, 3 and 4. While the catalyst did not show any activity yet after Experiment 2, the C_8 product composition for Experiment 3 was typical for a catalyst working properly according to a metal-catalyzed coordinative mechanism [3]. In contrast, Experiment 4 was stopped at a state in which the acid-catalyzed cationic mechanism was still prevailing. This is evident from the high fraction of dimethylhexene. Likewise, the C_8 composition after Experiment 1 also suggests a marked contribution of the cationic reaction pathway by the rather high percentage of dimethylhexene and the complete absence of n-octene. However, in contrast to Experiment 4, a Ni^+ EPR signal could be observed in the used catalyst of Experiment 1, although with slightly changed positions in comparison to the fresh one.

In Fig. 6A, EPR spectra of a 0.2Ni/SiAl-1(Cp) catalyst measured at 77 K after treating with 20 bar raffinate III at 353 K (solid lines) are plotted together with those of the freshly impregnated catalyst batch (dashed lines). It can be seen that only in Experiment 5 the fresh catalyst reveals the typical rhombic Ni^+ signal as shown in Fig. 4. This experiment was stopped after 48 h on stream, when the catalyst was widely deactivated. The raffinate III conversion was low, and the composition of the C_8 product fraction contained a high percentage of residual products comprising strongly branched molecules such as methylpentenes and higher oligomers up to C_{12} which point to a prevailing cationic mechanism. The Ni^+ signal present in the fresh catalyst disappeared, leaving behind a narrow line at 2.006 which may be due to carbon radicals in surface deposits. Experiment 6 was stopped after 24 h when the catalyst showed its optimum performance, and in the used catalyst an EPR signal was seen which reflects a superposition of contributions from different Ni^+ sites with slightly varying g tensor components. However, a very similar signal was also found after Experiment 7 which was stopped after 3 h when the catalyst did not show any activity. Inspection of Figs. 5 and 6 does not reveal any systematic relation between the catalytic performance and the appearance of the rhombic Ni^+ signal. The latter was found in both active and inactive states of the catalyst, while there were also both active and inactive states in which it was not present.

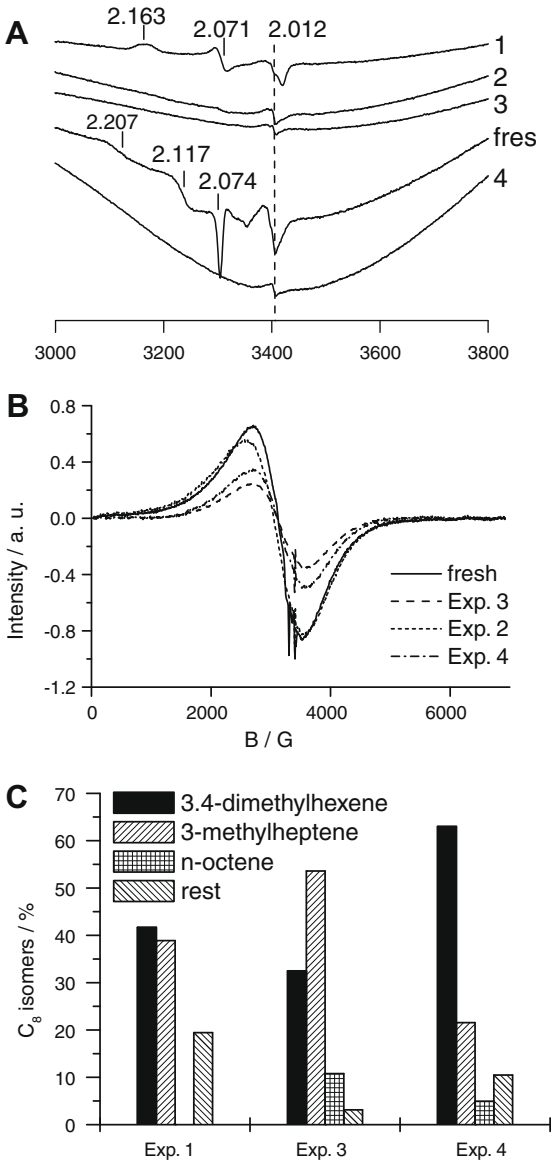

Fig. 5. EPR spectra of 0.3Ni/SiAl-1(COD) after different experiments in the middle field range (A) and in the total field range (B) and related composition of the C8 product fraction (C). The catalyst in Experiment 2 did not show any activity.

For the 0.3Ni/SiAl-1(COD) catalyst, a broad signal at $g = 2.26$ was observed from ferromagnetic Ni^0 clusters (Fig. 5B) already before exposure to raffinate III. This line remained almost unchanged after Experiment 2 which was shut down when the catalyst did not show any activity. However, a significant loss of signal intensity occurred after Experiment 3 in which the C_8 product distribution indicates that the catalyst was properly working in a metal-catalyzed coordinative mechanism. In comparison to this line, the Ni^0 cluster signal was higher after Experiment 4 in which the acid-catalyzed mechanism was still dominating as evident from the high percentage of dimethylhexenes and the missing n-octene.

In contrast, Ni^0 cluster formation was less pronounced for catalyst 0.2Ni/SiAl-1(Cp) prepared by impregnation with $Ni(Cp)_2$ (Fig. 6B). However, when this catalyst was held under reaction conditions until it started deactivating (Fig. 6, Experiment 5), a broad signal of ferromagnetic Ni^0 was also observed, although with a lower intensity than for 0.3Ni/SiAl-1(COD) (Fig. 5B, Experiment 5).

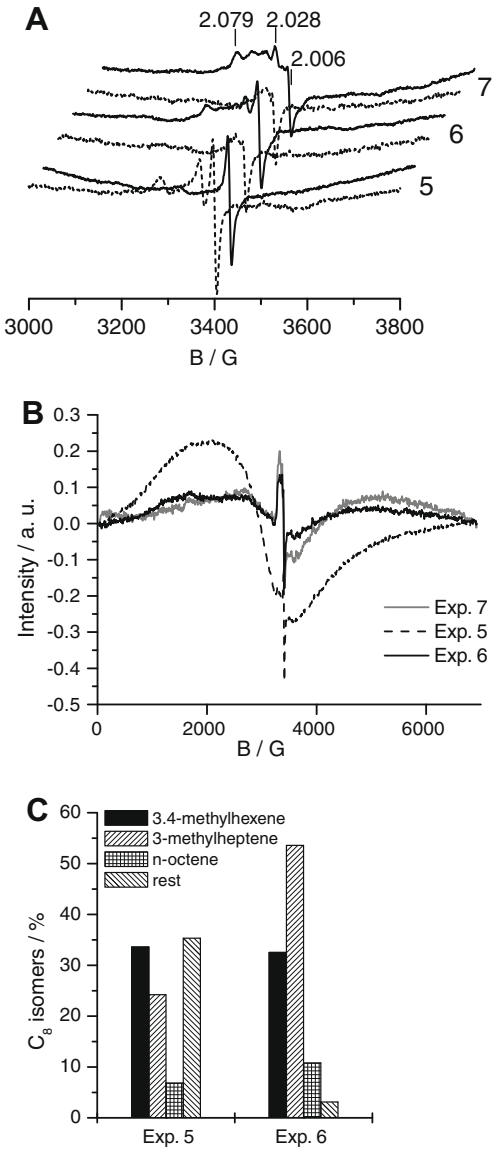

Fig. 6. EPR spectra of 0.2Ni/SiAl-1(Cp) after different experiments in the middle field range (A) and in the total field range (B) and related composition of the C8 product fraction (C). The catalyst in Experiment 7 did not show any activity.

In Fig. 7A and B, EPR spectra of the catalysts prepared with a Ni loading of 0.3% from $Ni(COD)_2$ on the two different supports are compared. The signal of ferromagnetic Ni^0 particles in catalyst 0.3Ni/SiAl-2(COD) on the less acidic support was broader and shifted to a higher *g*-value (Fig. 7A) which is almost the same as that observed for bulk Ni metal [18]. This suggests that the size and/or shape of the Ni^0 particles on SiAl-2 are slightly different from those of the Ni^0 particles on the more acidic SiAl-1 support. A Ni^+ signal with similar g tensor components was observed on both supports, although its intensity was lower on SiAl-2 (Fig. 7B). Under flowing raffinate III, catalyst 0.3Ni/SiAl-2(COD) became weakly active after about 8 h as evidenced by the slightly changing composition of the C4 fraction (Fig. 7C). The C8 fraction collected between 22 and 24 h time on stream showed a composition typical for the coordinative metal-catalyzed mechanism, however, the total amount of the collected C8 products was markedly lower than for the respective 0.3Ni/SiAl-1(COD) catalyst (Fig. 5, Experiment 3), and the Ni^+ signal present in the fresh 0.3Ni/SiAl-2(COD) catalyst disappeared after 24 h on stream, although the catalyst was still weakly active.

3.4. Surface acidity studied by FTIR spectroscopy of adsorbed pyridine

The relation between surface acidity and Ni loading was investigated by FTIR spectroscopy using pyridine as a probe molecule. A detailed description of the spectra including band assignment is given in the Supplementary material (Fig. S2). Briefly, all spectra showed a typical band of pyridinium ions PyH^+ at 1547 cm^{-1} formed by reaction with Brønsted sites, besides bands of pyridine adsorbed on Lewis sites at 1454 cm^{-1} and above 1600 cm^{-1}. The integrated Brønsted band intensity for SiAl-1 was almost three times as high as that for SiAl-2, indicating that SiAl-1 was much more acidic (Table 1). Moreover, Brønsted band intensities decreased with the Ni content. This is a clear evidence that Brønsted sites were consumed in the course of Ni bonding to the support surface. This process was accompanied by the appearance of a band of additional Lewis sites at 1608 cm^{-1} which most probably arose from Ni^{2+} [22]. Its intensity increased with the Ni loading (Supplementary material, Fig. S2). A very similar behaviour was observed for catalysts prepared using the same support SiAl-1 with the same Ni loading but with $Ni(COD)_2$ instead of $Ni(Cp)_2$ as the Ni source (Supplementary material, Fig. S3).

In contrast, pyridine adsorption on catalysts prepared from $Ni(COD)_2$ with the same loading of 0.2% Ni but on different supports revealed significant differences (Fig. 8). The intensity of the Brønsted band at 1545 cm^{-1} did not differ much for both catalysts. However, it has to be noted that the loss of Brønsted band area caused by depositing Ni on the support surface was much higher for SiAl-1. In this case, the area of the band at 1545 cm^{-1} dropped by 61% from 1.79 a.u. in the Ni-free support (Table 1) to 0.69 a.u. in 0.2% Ni/SiAl-1. In comparison, the Brønsted band in SiAl-2 lost only 12% of its area after deposition of 0.2% Ni, decreasing from 0.67 a.u. in the free support (Table 1) to 0.59 a.u. in the catalyst. Moreover, the ratios of the Lewis bands at 1609 cm^{-1} assigned to Ni^{2+} and at 1623 cm^{-1} assigned to Al^{3+} were markedly lower for 0.2% Ni/SiAl-2 (Fig. 8), i.e., relatively more Al^{3+} Lewis sites were detected on the latter catalyst. The reason could be a lower dispersion of Ni in this case.

4. Discussion

4.1. Influence of support, Ni source and Ni loading on the nature of Ni sites

In previous tests of a commercial NiO/SiAl-1 catalyst, the initial reaction period was governed by a change of an acid-catalyzed mechanism to a Ni-catalyzed mechanism, reflected by a change in the product composition [4]. This means that during this conditioning process, active Ni sites must be created from initially inactive Ni precursor species. The commercial NiO/SiAl-1 catalyst shows a broad EPR signal which is already present in the freshly calcined catalyst and which decreases slightly when the catalyst becomes active (Fig. 1). This suggests that the Ni precursors could be ferromagnetic Ni^0 clusters, which dissolve partly during conditioning to form active Ni species. Considering the observed change in the reaction mechanism [4], this process should go along with the consumption of Brønsted sites leading to reoxidation of Ni^0. A similar reaction was also observed for NiPd-containing zeolites (Eq. (2), [23])

$$Ni^0 + -OH \leftrightarrows -O-Ni^+H^-. \quad (2)$$

When strictly considered, conversion of a proton to a hydride species as depicted in Eq. (2) according to Ref. [23] would require transfer of two electrons, i.e., conversion of Ni^0 to Ni^{2+}. This would nicely agree with the FTIR spectra, in which the band at 1608 cm^{-1} reflects the formation of Ni^{2+} rather than of Ni^+ [22]. However, in Ni com-

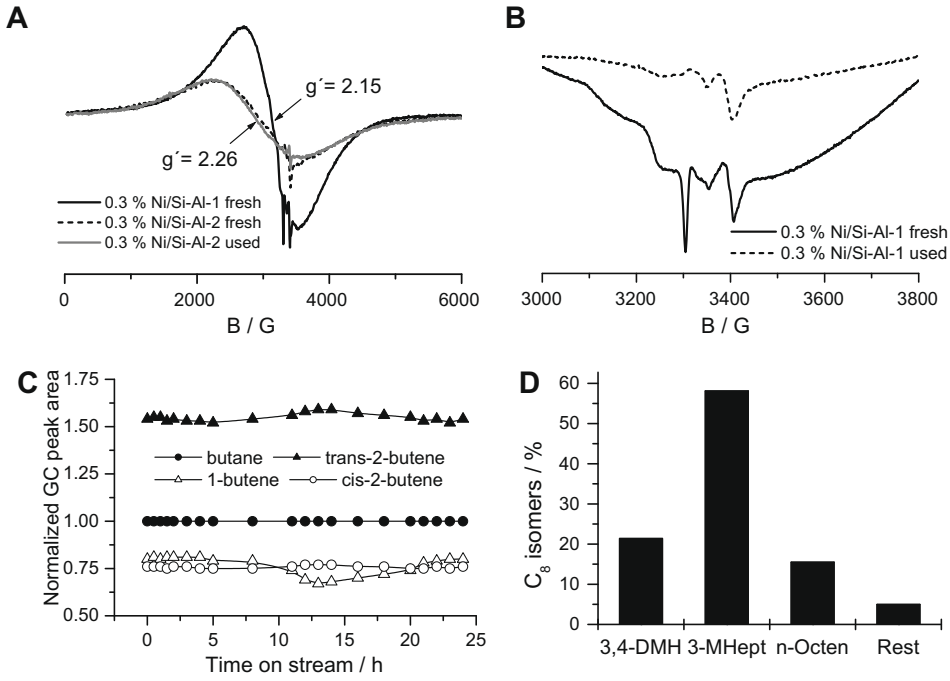

Fig. 7. (A and B) EPR spectra of the fresh and 24-h used 0.3Ni/SiAl-*x*(COD) catalysts. (C) on-line GC analysis of the C_4 fraction over 0.3Ni/SiAl-2(COD) plotted as relative peak areas $A/A_{n\text{-butane}}$, and (D) related composition of the C8 product fraction over 0.3Ni/SiAl-2(COD).

Table 1
Integrated intensities (a.u.) for the PyH^+ Brønsted bands.

	0.0% Ni	0.05% Ni	0.1% Ni	0.2% Ni	0.4% Ni
SiAl-1	1.79	0.86	0.77	0.65	0.33
SiAl-2	0.67	0.52	–	–	0.23

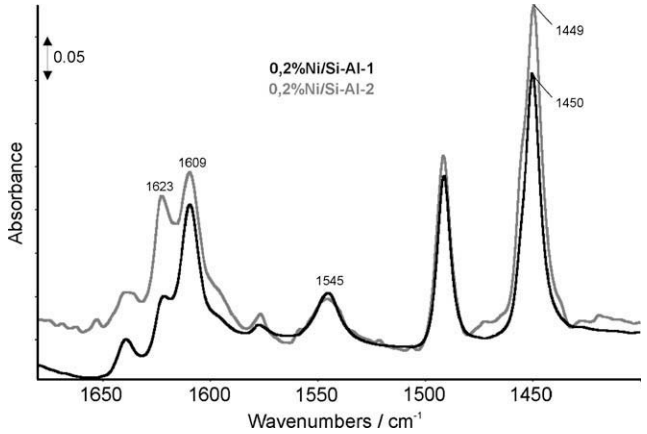

Fig. 8. Difference FTIR spectra of adsorbed pyridine at 373 K for 0.2Ni/SiAl-1(COD) and 0.2Ni/SiAl-2(COD).

plexes it is more realistic to assume partial charges, i.e., polar covalent rather than purely ionic bonding. This would also account for the formation of Ni^+, which is experimentally observed by EPR. Therefore, in the mechanistic discussion below, the reaction of Brønsted sites with Ni^0 is generally assumed to create Ni^{n+}.

More clear evidence for the fact that ferromagnetic Ni^0 clusters are not active in butene oligomerization is provided by operando EPR measurements performed on 6.0Ni/SiAl-1(Cp) (Fig. 2), which show that catalytic activity starts only after 5 h on stream, while the formation of ferromagnetic Ni^0 clusters by decomposition of the supported Ni complex is almost completed already after 90 min. Despite the lower Ni content and the fact that a considerable part of the Ni forms inactive Ni^0 clusters, this catalyst is even slightly more active than the industrial 20% NiO/SiAl-1 catalyst (compare Figs. 1B and 2B), suggesting that the active Ni component is a highly dispersed minority species.

This is also evident from CSTR tests, which were started with the pure support and in which the active catalyst was formed in situ by stepwise dosage of very low amounts of Ni (Fig. 3). After depositing about 3000 ppm Ni onto the SiAl-1 support by subsequently injecting portions of a 1% $Ni(COD)_2$/heptane solution into the feed stream, the catalyst showed a similar activity as the 20% NiO/SiAl-1 catalyst and the product composition became characteristic for a Ni-catalyzed mechanism (Fig. 3). This clearly shows that the active Ni site must be a minority species. Furthermore, the fact that the overall activity over the less acidic SiAl-2 support is markedly lower when the same Ni dosing procedure is applied supports the proposal in Eq. (2) that active Ni species are formed by reaction with Brønsted sites.

Additional information about the behaviour of acidic surface sites in contact with the Ni species is provided by FTIR spectroscopy of adsorbed pyridine. These results clearly show that Brønsted sites (band at 1547 cm^{-1}) are consumed and new Lewis sites (band at 1608 cm^{-1}) are formed when the Ni complexes are deposited on the support surface, and that the extent of this process is related to the concentration of Brønsted sites on the support (Fig. 8). Interestingly, very similar spectra and band intensities are observed for catalysts prepared with the same support and the same Ni loading but with complexes in which Ni takes different formal valence states, namely $Ni^0(COD)_2$ and $Ni^{2+}(Cp)_2$ (Supplementary material, Fig. S2). This suggests that the newly formed Lewis site is due to the same Ni species, probably a single Ni^{2+} site [22]. Again, this clearly confirms that Brønsted sites play a crucial role in the fixation of Ni single sites on the SiAl supports.

EPR measurements of the catalysts with a low Ni loading provide a deeper insight into the nature and behaviour of Ni sites formed upon impregnation of the supports with $Ni^{2+}(Cp)_2$ or Ni^0

$(COD)_2$. On both supports single Ni^+ sites are formed which, however, give rise to rather different EPR signals (Fig. 4B). In 0.3Ni/SiAl-1(Cp), the unusually low g_3 tensor value ($g_3 = 1.911$, Fig. 4B) suggests that the Cp ligand is still bound to the Ni site. It is well known that $Ni(Cp)_2$ can decompose to Ni^0 and $C_{10}H_{10}$ [24]. Possibly, this happens upon contact of $Ni(Cp)_2$ with the support surface, whereby the Ni^0 intermediate reacts further with a Brønsted surface site to form Ni^+, and $C_{10}H_{10}$ remains adsorbed in the vicinity of the Ni^+ site (Eq. (3)). The impregnation of the support has been repeated several times with different batches in the same way and with the same amount of $Ni(Cp)_2$ to check for the reproducibility of the Ni^+ EPR signal. It turned out that a Ni^+ signal was only observed in a part of the freshly prepared catalyst batches while some of them did not show it. This may be due to the relative stability of the $Ni(Cp)_2$ complex (Eq. (3))

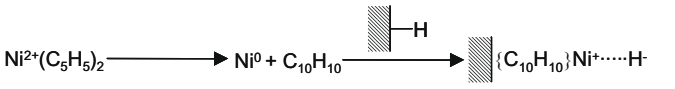

(3)

Another reason for the missing Ni^+ signal in some 0.3Ni/SiAl-1(Cp) batches could be that oxidation of Ni^0 by Brønsted sites as depicted in Eq. (3) does not stop at monovalent Ni^+, but can also produce a certain amount of Ni^{2+} being EPR-silent under these conditions. This would agree with the FTIR results of pyridine adsorption, in which a band at 1608 cm^{-1} suggests the formation of Ni^{2+} Lewis sites in all catalysts, which is independent on the kind of the Ni complex used for preparation.

For the Ni^+ signal in 0.3Ni/SiAl-1(COD), all g tensor components are larger than $g_e = 2.0023$, as expected for Ni^+ (Fig. 4B). As for $Ni(Cp)_2$, different catalyst batches have been prepared in the same way with the same loading of $Ni(COD)_2$. In contrast to 0.3Ni/SiAl-1(Cp), all freshly prepared 0.3Ni/SiAl-1(COD) batches showed the same Ni^+ signal. Obviously, $Ni(COD)_2$ as a Ni^0 compound is less stable than $Ni(Cp)_2$ when it is adsorbed on the acidic SiAl-1 support and decomposes readily by the release of C_8H_{12} (Eq. (4))

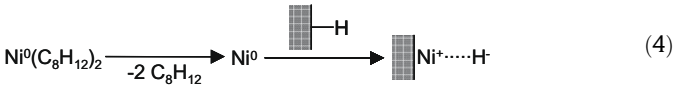

(4)

In accordance with the FTIR results, the mechanisms proposed in Eqs. (3) and (4) account for the observed consumption of Brønsted sites.

As described in Section 3.3 and deduced from Figs. 5 and 6, no systematic relation between the catalytic performance and the Ni^+ signal in the EPR spectra could be found. This suggests that the highly stable EPR-active Ni^+ species in this work and probably also the Ni^+ species with similar g tensor components detected by EPR in previous investigations [10–14] are spectator species.

CSTR tests have shown that the catalysts deactivate upon prolonged use whereby they lose not only activity but also selectivity. This means that branched products formed by acidic catalysis are again gradually increasing upon extended times on stream. When the in situ EPR spectra of catalyst 0.2Ni/SiAl-1(Cp) is compared with the related product compositions, a broad signal of ferromagnetic Ni^0 clusters is evident after partial deactivation (Fig. 6, Experiment 5), which is not seen when the catalyst is still working properly (Fig. 6, Experiment 6). This suggests that deactivation goes along with the agglomeration of dispersed Ni sites which in turn should recreate acidic surface sites, as suggested by the gradual change of the C_8 product composition from being typical for a metal-catalyzed coordinative reaction mechanism to an acid-catalyzed cationic reaction mechanism (Fig. 6C).

Summarizing the behaviour in Figs. 5B and 6B, it appears that Ni^0 clusters, if present in the freshly impregnated catalyst, are obviously dissolved as the catalyst is becoming active, pass a minimum when the catalyst is working at its optimum performance and reaggregate again upon deactivation. Since this behaviour goes along with a change in the C_8product composition, it is probable that the acidic surface sites play a crucial role insofar as they are consumed during conditioning by creating highly dispersed Ni single sites and set free during deactivation as a consequence of reaggregation of these single sites. The lower overall activity and faster deactivation of the catalysts based on the less acidic support SiAl-2 (Supplementary material, Fig. S1) may be due to the insufficient number of Brønsted sites available to keep the Ni sites isolated.

5. Conclusions

An industrial 20% $NiO/SiO_2–Al_2O_3$catalyst as well as a series of supported $Ni/SiO_2–Al_2O_3$ catalysts with Ni loadings between 0.2% and 6% prepared by impregnation of two differently acidic supports with $Ni(Cp)_2$ and $Ni(COD)_2$ complexes has been studied by EPR spectroscopy either under reaction conditions at 353 K and at 20 bar raffinate III and/or after quenching for the first time. These experiments clearly show that ferromagnetic Ni^0 clusters formed in certain catalysts depending on Ni precursor and loading are catalytically inactive. When initially present in fresh catalysts, these clusters dissolve partly to form Ni single sites, which govern the catalytic activity. Upon deactivation, the latter reaggregate again and restore the inactive Ni^0 clusters.

Brønsted sites play a crucial role in the formation of active sites and the nature of the catalytic mechanism. They dominate as active sites at the start of the reaction, giving rise to a cationic mechanism which leads to undesired strongly branched products. During subsequent conditioning they are consumed by oxidative addition to Ni^0 and create active Ni^{n+} species. This is connected with a change of the catalytic mechanism and, consequently, of the product composition from strongly branched olefins to more linear olefins.

There is no doubt that single Ni^{n+} species are active sites for the metal-catalyzed mechanism leading to the desired more linear olefins. However, the stable Ni^+ species, which are detectable by EPR and which are likewise also found in other systems [9–13], are most probably only spectator species since no clear relation between the catalytic performance and the appearance of these sites was found. Taking into account that the product composition over optimized heterogeneous Ni catalysts [4] is very similar to that obtained from homogeneous process, which is considered to proceed on Ni^{n+}–H sites via subsequent butene insertion into the Ni–H bond followed by β-H elimination of octene [5–8], it is possible that the EPR-active Ni^+ spectator species in the solid catalysts are part of stable alkyl complexes which are unable to undergo β-H elimination or transfer to deliberate olefin and enter into a new reaction cycle. The reason that active Ni species are not detected by EPR could be a rapid change of their coordination symmetry which reduces their transient life time and/or their presence as EPR-silent Ni^{2+}.

In summary, it can be concluded that, apart from the fact that they escape direct detection by in situ EPR, active sites consist of single Ni^{n+} ($n = 1$ and/or 2) moieties which are formed by reaction of Ni^0 precursor species with Brønsted sites in the conditioning period and destroyed by reaggregation to Ni^0 clusters during deactivation.

Appendix A. Supplementary material

Supplementary data associated with this article can be found, in the online version, at doi:10.1016/j.jcat.2009.05.021.

References

[1] US 2.581.228, Phillips Petroleum, applied 1945-06-15, continuation of Application No. 435.888 filed 1942-03-23.
[2] S. Albrecht, D. Kießling, D. Maschmeyer, F. Nierlich, G. Wendt, Chem. Eng. Technol. 77 (2007) 695.
[3] G. Wendt, D. Kießling, Chem. Technol. 47 (1995) 136.
[4] P. Albers, U. Bentrup, A. Brückner, F. Nierlich, H.-W. Zanthoff, D. Maschmeyer, DGMK-Tagungsbericht 2004-3, ISBN 3-936418-23-3.
[5] L.C. Simon, J. Dupont, R.F. de Souza, Appl. Catal. A: Gen. 175 (1998) 215.
[6] Y. Chauvin, H. Olivier, C.N. Wyrvalski, L.C. Simon, R.F. de Souza, J. Catal. 165 (1997) 275.
[7] V.V. Saraev, P.B. Kraikivskii, S.N. Zelinskii, G.V. Ratovskii, V.S. Tkach, F.K. Shmidt, Russ. J. Coord. Chem. 27 (2001) 757.
[8] M.C. Leatherman, M. Brookhart, Macromolecules 34 (2001) 2748.
[9] G. Wendt, J. Finster, R. Schoellner, H. Siegel, Stud. Surf. Sci. Catal. 7 (1981) 978.
[10] A. Barth, R. Kirmse, J. Stach, Z. Chem. 24 (1984) 195.
[11] I.V. Elev, B.N. Shelimov, V.B. Kazanski, J. Catal. 89 (1984) 470.
[12] L. Bonneviot, D. Olivier, M. Che, J. Mol. Catal. 21 (1983) 415.
[13] K. Dyrek, D. Kiessling, M. Labanowska, G. Wendt, J. Widziszewska, Colloids Surfaces: Physicochem. Eng. Aspects 72 (1993) 183.
[14] T. Cai, Catal. Today 51 (1999) 153.
[15] T. Yashima, Y. Ushida, M. Ebisawa, N. Hara, J. Catal. 36 (1975) 320.
[16] A. Brückner, Chem. Commun. 13 (2005) 1761.
[17] G.P. Lozos, B.M. Hofman, C.G. Franz, Quantum Chemistry Programs Exchange (265) (1973).
[18] P.A. Jacobs, H. Nijs, J. Verdonck, E.D. Derouane, J.-P. Gilson, A.J. Simoens, J. Chem. Soc., Faraday Trans. I 75 (1979) 1196.
[19] J.R. Pilbrow, Transition Ion Electron Paramagnetic Resonance, Clarendon Press, Oxford, 1990, p. 154 ff.
[20] V.V. Saraev, P.B. Kraikivskii, V.V. Annenkov, S.N. Zelinskiy, D.A. Matveev, A.I. Vilms, E.N. Danilovtseva, K. Lammertsma, ARKIVOC 15 (2005) 4.
[21] A. Klein, A. Kaiser, B. Sarkar, M. Wanner, J. Fiedler, Eur. J. Inorg. Chem. (2007) 965.
[22] G. Busca, Catal. Today 41 (1998) 191.
[23] J.S. Feely, W.M.H. Sachtler, Zeolites 10 (1990) 739.
[24] L.M. Dyagileva, E.I. Tsyganova, Y.A. Aleksandrov, Russ. Chem. Rev. 57 (1988) 316.